Measurement of the Single-Top-Quark Production Cross Section at CDF

T. Aaltonen,[24] J. Adelman,[14] T. Akimoto,[56] M. G. Albrow,[18] B. Álvarez González,[12] S. Amerio,[44a,44b] D. Amidei,[35] A. Anastassov,[39] A. Annovi,[20] J. Antos,[15] G. Apollinari,[18] A. Apresyan,[49] T. Arisawa,[58] A. Artikov,[16] W. Ashmanskas,[18] A. Attal,[4] A. Aurisano,[54] F. Azfar,[43] P. Azzurri,[47a,47d] W. Badgett,[18] A. Barbaro-Galtieri,[29] V. E. Barnes,[49] B. A. Barnett,[26] V. Bartsch,[31] G. Bauer,[33] P.-H. Beauchemin,[34] F. Bedeschi,[47a] P. Bednar,[15] D. Beecher,[31] S. Behari,[26] G. Bellettini,[47a,47b] J. Bellinger,[60] D. Benjamin,[17] A. Beretvas,[18] J. Beringer,[29] A. Bhatti,[51] M. Binkley,[18] D. Bisello,[44a,44b] I. Bizjak,[31] R. E. Blair,[2] C. Blocker,[7] B. Blumenfeld,[26] A. Bocci,[17] A. Bodek,[50] V. Boisvert,[50] G. Bolla,[49] D. Bortoletto,[49] J. Boudreau,[48] A. Boveia,[11] B. Brau,[11] A. Bridgeman,[25] L. Brigliadori,[44a] C. Bromberg,[36] E. Brubaker,[14] J. Budagov,[16] H. S. Budd,[50] S. Budd,[25] K. Burkett,[18] G. Busetto,[44a,44b] P. Bussey,[22] A. Buzatu,[34] K. L. Byrum,[2] S. Cabrera,[17,q] C. Calancha,[32] M. Campanelli,[36] M. Campbell,[35] F. Canelli,[18] A. Canepa,[46] D. Carlsmith,[60] R. Carosi,[47a] S. Carrillo,[19,k] S. Carron,[34] B. Casal,[12] M. Casarsa,[18] A. Castro,[6a,6b] P. Catastini,[47a,47c] D. Cauz,[55a,55b] V. Cavaliere,[47a,47c] M. Cavalli-Sforza,[4] A. Cerri,[29] L. Cerrito,[31,o] S. H. Chang,[28] Y. C. Chen,[1] M. Chertok,[8] G. Chiarelli,[47a] G. Chlachidze,[18] F. Chlebana,[18] K. Cho,[28] D. Chokheli,[16] J. P. Chou,[23] G. Choudalakis,[33] S. H. Chuang,[53] K. Chung,[13] W. H. Chung,[60] Y. S. Chung,[50] C. I. Ciobanu,[45] M. A. Ciocci,[47a,47c] A. Clark,[21] D. Clark,[7] G. Compostella,[44a] M. E. Convery,[18] J. Conway,[8] K. Copic,[35] M. Cordelli,[20] G. Cortiana,[44a,44b] D. J. Cox,[8] F. Crescioli,[47a,47b] C. Cuenca Almenar,[8,q] J. Cuevas,[12,n] R. Culbertson,[18] J. C. Cully,[35] D. Dagenhart,[18] M. Datta,[18] T. Davies,[22] P. de Barbaro,[50] S. De Cecco,[52a] A. Deisher,[29] G. De Lorenzo,[4] M. Dell'Orso,[47a,47b] C. Deluca,[4] L. Demortier,[51] J. Deng,[17] M. Deninno,[6a] P. F. Derwent,[18] G. P. di Giovanni,[45] C. Dionisi,[52a,52b] B. Di Ruzza,[55a,55b] J. R. Dittmann,[5] M. D'Onofrio,[4] S. Donati,[47a,47b] P. Dong,[9] J. Donini,[44a] T. Dorigo,[44a] S. Dube,[53] J. Efron,[40] A. Elagin,[54] R. Erbacher,[8] D. Errede,[25] S. Errede,[25] R. Eusebi,[18] H. C. Fang,[29] S. Farrington,[43] W. T. Fedorko,[14] R. G. Feild,[61] M. Feindt,[27] J. P. Fernandez,[32] C. Ferrazza,[47a,47d] R. Field,[19] G. Flanagan,[49] R. Forrest,[8] M. Franklin,[23] J. C. Freeman,[18] I. Furic,[19] M. Gallinaro,[52a] J. Galyardt,[13] F. Garberson,[11] J. E. Garcia,[47a] A. F. Garfinkel,[49] K. Genser,[18] H. Gerberich,[25] D. Gerdes,[35] A. Gessler,[27] S. Giagu,[52a,52b] V. Giakoumopoulou,[3] P. Giannetti,[47a] K. Gibson,[48] J. L. Gimmell,[50] C. M. Ginsburg,[18] N. Giokaris,[3] M. Giordani,[55a,55b] P. Giromini,[20] M. Giunta,[47a,47b] G. Giurgiu,[26] V. Glagolev,[16] D. Glenzinski,[18] M. Gold,[38] N. Goldschmidt,[19] A. Golossanov,[18] G. Gomez,[12] G. Gomez-Ceballos,[33] M. Goncharov,[54] O. González,[32] I. Gorelov,[38] A. T. Goshaw,[17] K. Goulianos,[51] A. Gresele,[44a,44b] S. Grinstein,[23] C. Grosso-Pilcher,[14] R. C. Group,[18] U. Grundler,[25] J. Guimaraes da Costa,[23] Z. Gunay-Unalan,[36] C. Haber,[29] K. Hahn,[33] S. R. Hahn,[18] E. Halkiadakis,[53] B.-Y. Han,[50] J. Y. Han,[50] R. Handler,[60] F. Happacher,[20] K. Hara,[56] D. Hare,[53] M. Hare,[57] S. Harper,[43] R. F. Harr,[59] R. M. Harris,[18] M. Hartz,[48] K. Hatakeyama,[51] J. Hauser,[9] C. Hays,[43] M. Heck,[27] A. Heijboer,[46] B. Heinemann,[29] J. Heinrich,[46] C. Henderson,[33] M. Herndon,[60] J. Heuser,[27] S. Hewamanage,[5] D. Hidas,[17] C. S. Hill,[11,d] D. Hirschbuehl,[27] A. Hocker,[18] S. Hou,[1] M. Houlden,[30] S.-C. Hsu,[10] B. T. Huffman,[43] R. E. Hughes,[40] U. Husemann,[61] J. Huston,[36] J. Incandela,[11] G. Introzzi,[47a] M. Iori,[52a,52b] A. Ivanov,[8] E. James,[18] B. Jayatilaka,[17] E. J. Jeon,[28] M. K. Jha,[6a] S. Jindariani,[18] W. Johnson,[8] M. Jones,[49] K. K. Joo,[28] S. Y. Jun,[13] J. E. Jung,[28] T. R. Junk,[18] T. Kamon,[54] D. Kar,[19] P. E. Karchin,[59] Y. Kato,[42] R. Kephart,[18] J. Keung,[46] V. Khotilovich,[54] B. Kilminster,[40] D. H. Kim,[28] H. S. Kim,[28] J. E. Kim,[28] M. J. Kim,[20] S. B. Kim,[28] S. H. Kim,[56] Y. K. Kim,[14] N. Kimura,[56] L. Kirsch,[7] S. Klimenko,[19] B. Knuteson,[33] B. R. Ko,[17] S. A. Koay,[11] K. Kondo,[58] D. J. Kong,[28] J. Konigsberg,[19] A. Korytov,[19] A. V. Kotwal,[17] M. Kreps,[27] J. Kroll,[46] D. Krop,[14] N. Krumnack,[5] M. Kruse,[17] V. Krutelyov,[11] T. Kubo,[56] T. Kuhr,[27] N. P. Kulkarni,[59] M. Kurata,[56] Y. Kusakabe,[58] S. Kwang,[14] A. T. Laasanen,[49] S. Lami,[47a] S. Lammel,[18] M. Lancaster,[31] R. L. Lander,[8] K. Lannon,[40] A. Lath,[53] G. Latino,[47a,47c] I. Lazzizzera,[44a,44b] T. LeCompte,[2] E. Lee,[54] H. S. Lee,[14] S. W. Lee,[54,p] S. Leone,[47a] J. D. Lewis,[18] C. S. Lin,[29] J. Linacre,[43] M. Lindgren,[18] E. Lipeles,[10] T. M. Liss,[25] A. Lister,[8] D. O. Litvintsev,[18] C. Liu,[48] T. Liu,[18] N. S. Lockyer,[46] A. Loginov,[61] M. Loreti,[44a,44b] L. Lovas,[15] R.-S. Lu,[1] D. Lucchesi,[44a,44b] J. Lueck,[27] C. Luci,[52a,52b] P. Lujan,[29] P. Lukens,[18] G. Lungu,[51] L. Lyons,[43] J. Lys,[29] R. Lysak,[15] E. Lytken,[49] P. Mack,[27] D. MacQueen,[34] R. Madrak,[18] K. Maeshima,[18] K. Makhoul,[33] T. Maki,[24] P. Maksimovic,[26] S. Malde,[43] S. Malik,[31] G. Manca,[30,r] A. Manousakis-Katsikakis,[3] F. Margaroli,[49] C. Marino,[27] C. P. Marino,[25] A. Martin,[61] V. Martin,[22,j] M. Martínez,[4] R. Martínez-Ballarín,[32] T. Maruyama,[56] P. Mastrandrea,[52a] T. Masubuchi,[56] M. E. Mattson,[59] P. Mazzanti,[6a] K. S. McFarland,[50] P. McIntyre,[54] R. McNulty,[30,i] A. Mehta,[30] P. Mehtala,[24] A. Menzione,[47a] P. Merkel,[49] C. Mesropian,[51] T. Miao,[18] N. Miladinovic,[7] R. Miller,[36] C. Mills,[23] M. Milnik,[27] A. Mitra,[1] G. Mitselmakher,[19] H. Miyake,[56] N. Moggi,[6a] C. S. Moon,[28] R. Moore,[18] M. J. Morello,[47a,47b] J. Morlok,[27] P. Movilla Fernandez,[18] J. Mülmenstädt,[29] A. Mukherjee,[18] Th. Muller,[27] R. Mumford,[26] P. Murat,[18] M. Mussini,[6a,6b] J. Nachtman,[18] Y. Nagai,[56] A. Nagano,[56] J. Naganoma,[58] K. Nakamura,[56] I. Nakano,[41]

A. Napier,[57] V. Necula,[17] C. Neu,[46] M. S. Neubauer,[25] J. Nielsen,[29,f] L. Nodulman,[2] M. Norman,[10] O. Norniella,[25] E. Nurse,[31] L. Oakes,[43] S. H. Oh,[17] Y. D. Oh,[28] I. Oksuzian,[19] T. Okusawa,[42] R. Orava,[24] K. Osterberg,[24] S. Pagan Griso,[44a,44b] C. Pagliarone,[47a] E. Palencia,[18] V. Papadimitriou,[18] A. Papaikonomou,[27] A. A. Paramonov,[14] B. Parks,[40] S. Pashapour,[34] J. Patrick,[18] G. Pauletta,[55a,55b] M. Paulini,[13] C. Paus,[33] T. Peiffer,[27] D. E. Pellett,[8] A. Penzo,[55a] T. J. Phillips,[17] G. Piacentino,[47a] E. Pianori,[46] L. Pinera,[19] K. Pitts,[25] C. Plager,[9] L. Pondrom,[60] O. Poukhov,[16,a] N. Pounder,[43] F. Prakoshyn,[16] A. Pronko,[18] J. Proudfoot,[2] F. Ptohos,[18,h] E. Pueschel,[13] G. Punzi,[47a,47b] J. Pursley,[60] J. Rademacker,[43,d] A. Rahaman,[48] V. Ramakrishnan,[60] N. Ranjan,[49] I. Redondo,[32] B. Reisert,[18] V. Rekovic,[38] P. Renton,[43] M. Renz,[27] M. Rescigno,[52a] S. Richter,[27] F. Rimondi,[6a,6b] L. Ristori,[47a] A. Robson,[22] T. Rodrigo,[12] T. Rodriguez,[46] E. Rogers,[25] S. Rolli,[57] R. Roser,[18] M. Rossi,[55a] R. Rossin,[11] P. Roy,[34] A. Ruiz,[12] J. Russ,[13] V. Rusu,[18] H. Saarikko,[24] A. Safonov,[54] W. K. Sakumoto,[50] O. Saltó,[4] L. Santi,[55a,55b] S. Sarkar,[52a,52b] L. Sartori,[47a] K. Sato,[18] A. Savoy-Navarro,[45] I. Schall,[27] T. Scheidle,[27] P. Schlabach,[18] A. Schmidt,[27] E. E. Schmidt,[18] M. A. Schmidt,[14] M. P. Schmidt,[61,a] M. Schmitt,[39] T. Schwarz,[8] L. Scodellaro,[12] A. L. Scott,[11] A. Scribano,[47a,47c] F. Scuri,[47a] A. Sedov,[49] S. Seidel,[38] Y. Seiya,[42] A. Semenov,[16] L. Sexton-Kennedy,[18] A. Sfyrla,[21] S. Z. Shalhout,[59] T. Shears,[30] P. F. Shepard,[48] D. Sherman,[23] M. Shimojima,[56,m] S. Shiraishi,[14] M. Shochet,[14] Y. Shon,[60] I. Shreyber,[37] A. Sidoti,[47a] P. Sinervo,[34] A. Sisakyan,[16] A. J. Slaughter,[18] J. Slaunwhite,[40] K. Sliwa,[57] J. R. Smith,[8] F. D. Snider,[18] R. Snihur,[34] A. Soha,[8] S. Somalwar,[53] V. Sorin,[36] J. Spalding,[18] T. Spreitzer,[34] P. Squillacioti,[47a,47c] M. Stanitzki,[61] R. St. Denis,[22] B. Stelzer,[9] O. Stelzer-Chilton,[43] D. Stentz,[39] J. Strologas,[38] D. Stuart,[11] J. S. Suh,[28] A. Sukhanov,[19] I. Suslov,[16] T. Suzuki,[56] A. Taffard,[25,e] R. Takashima,[41] Y. Takeuchi,[56] R. Tanaka,[41] M. Tecchio,[35] P. K. Teng,[1] K. Terashi,[51] J. Thom,[18,g] A. S. Thompson,[22] G. A. Thompson,[25] E. Thomson,[46] P. Tipton,[61] V. Tiwari,[13] S. Tkaczyk,[18] D. Toback,[54] S. Tokar,[15] K. Tollefson,[36] T. Tomura,[56] D. Tonelli,[18] S. Torre,[20] D. Torretta,[18] P. Totaro,[55a,55b] S. Tourneur,[45] Y. Tu,[46] N. Turini,[47a,47c] F. Ukegawa,[56] S. Vallecorsa,[21] N. van Remortel,[24,b] A. Varganov,[35] E. Vataga,[47a,47d] F. Vázquez,[19,k] G. Velev,[18] C. Vellidis,[3] V. Veszpremi,[49] M. Vidal,[32] R. Vidal,[18] I. Vila,[12] R. Vilar,[12] T. Vine,[31] M. Vogel,[38] I. Volobouev,[29,p] G. Volpi,[47a,47b] F. Würthwein,[10] P. Wagner,[54] R. G. Wagner,[2] R. L. Wagner,[18] J. Wagner-Kuhr,[27] W. Wagner,[27] T. Wakisaka,[42] R. Wallny,[9] S. M. Wang,[1] A. Warburton,[34] D. Waters,[31] M. Weinberger,[54] W. C. Wester III,[18] B. Whitehouse,[57] D. Whiteson,[46,e] A. B. Wicklund,[2] E. Wicklund,[18] G. Williams,[34] H. H. Williams,[46] P. Wilson,[18] B. L. Winer,[40] P. Wittich,[18,g] S. Wolbers,[18] C. Wolfe,[14] T. Wright,[35] X. Wu,[21] S. M. Wynne,[30] S. Xie,[33] A. Yagil,[10] K. Yamamoto,[42] J. Yamaoka,[53] U. K. Yang,[14,l] Y. C. Yang,[28] W. M. Yao,[29] G. P. Yeh,[18] J. Yoh,[18] K. Yorita,[14] T. Yoshida,[42] G. B. Yu,[50] I. Yu,[28] S. S. Yu,[18] J. C. Yun,[18] L. Zanello,[52a,52b] A. Zanetti,[55a] I. Zaw,[23] X. Zhang,[25] Y. Zheng,[9,c] and S. Zucchelli[6a,6b]

(CDF Collaboration)

[1]*Institute of Physics, Academia Sinica, Taipei, Taiwan 11529, Republic of China*
[2]*Argonne National Laboratory, Argonne, Illinois 60439, USA*
[3]*University of Athens, 157 71 Athens, Greece*
[4]*Institut de Fisica d'Altes Energies, Universitat Autonoma de Barcelona, E-08193, Bellaterra (Barcelona), Spain*
[5]*Baylor University, Waco, Texas 76798, USA*
[6a]*Istituto Nazionale di Fisica Nucleare Bologna, I-40127 Bologna, Italy;*
[6b]*University of Bologna, I-40127 Bologna, Italy*
[7]*Brandeis University, Waltham, Massachusetts 02254, USA*
[8]*University of California, Davis, Davis, California 95616, USA*
[9]*University of California, Los Angeles, Los Angeles, California 90024, USA*
[10]*University of California, San Diego, La Jolla, California 92093, USA*
[11]*University of California, Santa Barbara, Santa Barbara, California 93106, USA*
[12]*Instituto de Fisica de Cantabria, CSIC-University of Cantabria, 39005 Santander, Spain*
[13]*Carnegie Mellon University, Pittsburgh, Pennsylvania 15213, USA*
[14]*Enrico Fermi Institute, University of Chicago, Chicago, Illinois 60637, USA*
[15]*Comenius University, 842 48 Bratislava, Slovakia; Institute of Experimental Physics, 040 01 Kosice, Slovakia*
[16]*Joint Institute for Nuclear Research, RU-141980 Dubna, Russia*
[17]*Duke University, Durham, North Carolina 27708, USA*
[18]*Fermi National Accelerator Laboratory, Batavia, Illinois 60510, USA*
[19]*University of Florida, Gainesville, Florida 32611, USA*
[20]*Laboratori Nazionali di Frascati, Istituto Nazionale di Fisica Nucleare, I-00044 Frascati, Italy*
[21]*University of Geneva, CH-1211 Geneva 4, Switzerland*
[22]*Glasgow University, Glasgow G12 8QQ, United Kingdom*
[23]*Harvard University, Cambridge, Massachusetts 02138, USA*

[24]Division of High Energy Physics, Department of Physics, University of Helsinki and Helsinki Institute of Physics, FIN-00014, Helsinki, Finland
[25]University of Illinois, Urbana, Illinois 61801, USA
[26]The Johns Hopkins University, Baltimore, Maryland 21218, USA
[27]Institut für Experimentelle Kernphysik, Universität Karlsruhe, 76128 Karlsruhe, Germany
[28]Center for High-Energy Physics: Kyungpook National University, Daegu 702-701, Korea; Seoul National University, Seoul 151-742, Korea; Sungkyunkwan University, Suwon 440-746, Korea; Korea Institute of Science and Technology Information, Daejeon, 305-806, Korea; Chonnam National University, Gwangju, 500-757, Korea
[29]Ernest Orlando Lawrence Berkeley National Laboratory, Berkeley, California 94720, USA
[30]University of Liverpool, Liverpool L69 7ZE, United Kingdom
[31]University College London, London WC1E 6BT, United Kingdom
[32]Centro de Investigaciones Energeticas Medioambientales y Tecnologicas, E-28040 Madrid, Spain
[33]Massachusetts Institute of Technology, Cambridge, Massachusetts 02139, USA
[34]Institute of Particle Physics: McGill University, Montréal, Canada H3A 2T8; and University of Toronto, Toronto, Canada M5S 1A7
[35]University of Michigan, Ann Arbor, Michigan 48109, USA
[36]Michigan State University, East Lansing, Michigan 48824, USA
[37]Institution for Theoretical and Experimental Physics, ITEP, Moscow 117259, Russia
[38]University of New Mexico, Albuquerque, New Mexico 87131, USA
[39]Northwestern University, Evanston, Illinois 60208, USA
[40]The Ohio State University, Columbus, Ohio 43210, USA
[41]Okayama University, Okayama 700-8530, Japan
[42]Osaka City University, Osaka 588, Japan
[43]University of Oxford, Oxford OX1 3RH, United Kingdom
[44a]Istituto Nazionale di Fisica Nucleare, Sezione di Padova-Trento, I-35131 Padova, Italy;
[44b]University of Padova, I-35131 Padova, Italy
[45]LPNHE, Universite Pierre et Marie Curie/IN2P3-CNRS, UMR7585, Paris, F-75252 France
[46]University of Pennsylvania, Philadelphia, Pennsylvania 19104, USA
[47a]Istituto Nazionale di Fisica Nucleare Pisa, I-56127 Pisa, Italy;
[47b]University of Pisa, I-56127 Pisa, Italy;
[47c]University of Siena, I-56127 Pisa, Italy;
[47d]Scuola Normale Superiore, I-56127 Pisa, Italy
[48]University of Pittsburgh, Pittsburgh, Pennsylvania 15260, USA
[49]Purdue University, West Lafayette, Indiana 47907, USA
[50]University of Rochester, Rochester, New York 14627, USA
[51]The Rockefeller University, New York, New York 10021, USA
[52a]Istituto Nazionale di Fisica Nucleare, Sezione di Roma 1, I-00185 Roma, Italy;
[52b]Sapienza Università di Roma, I-00185 Roma, Italy
[53]Rutgers University, Piscataway, New Jersey 08855, USA
[54]Texas A&M University, College Station, Texas 77843, USA
[55a]Istituto Nazionale di Fisica Nucleare Trieste/Udine, Italy;
[55b]University of Trieste/Udine, Italy
[56]University of Tsukuba, Tsukuba, Ibaraki 305, Japan
[57]Tufts University, Medford, Massachusetts 02155, USA
[58]Waseda University, Tokyo 169, Japan
[59]Wayne State University, Detroit, Michigan 48201, USA
[60]University of Wisconsin, Madison, Wisconsin 53706, USA
[61]Yale University, New Haven, Connecticut 06520, USA

(Received 16 September 2008; published 15 December 2008)

We report a measurement of the single-top-quark production cross section in 2.2 fb^{-1} of $p\bar{p}$ collision data collected by the Collider Detector at Fermilab at $\sqrt{s} = 1.96$ TeV. Candidate events are classified as signal-like by three parallel analyses which use likelihood, matrix element, and neural network discriminants. These results are combined in order to improve the sensitivity. We observe a signal consistent with the standard model prediction, but inconsistent with the background-only model by 3.7 standard deviations with a median expected sensitivity of 4.9 standard deviations. We measure a cross section of $2.2^{+0.7}_{-0.6}$(stat + syst) pb, extract the Cabibbo-Kobayashi-Maskawa matrix-element value $|V_{tb}| = 0.88^{+0.13}_{-0.12}$(stat + syst) $\pm$ 0.07(theory), and set the limit $|V_{tb}| > 0.66$ at the 95% C.L.

DOI: 10.1103/PhysRevLett.101.252001 PACS numbers: 14.65.Ha, 12.15.Hh, 12.15.Ji, 13.85.Qk

The top quark was discovered by the CDF and D0 collaborations in 1995 [1] in the strong interaction $p\bar{p} \rightarrow t\bar{t} + X$. Since then, a comprehensive program of measurements has brought more precise knowledge of the top quark's mass, pair-production cross section, and a number of its decay properties [2]. The evidence strongly suggests that the particle observed in 1995 is the $SU(2)$ partner of the bottom quark and that it decays nearly 100% of the time into Wb with a very short lifetime. The weak couplings of the top quark are less well constrained, except that $|V_{tb}|^2 \gg |V_{td}|^2 + |V_{ts}|^2$ [3]. Requiring that the 3×3 Cabibbo-Kobayashi-Maskawa (CKM) matrix is unitary implies that $|V_{tb}| \simeq 1$ [2]. With a matrix of higher rank, though, $|V_{tb}|$ could be small without measurably changing the $t \rightarrow Wb$ branching ratio. Production of single top quarks provides a direct measurement of $|V_{tb}|$ and a test of the b-quark content of the proton.

Top quarks are expected to be produced singly, as shown in Fig. 1. The combined $s + t$-channel cross section is predicted at next-to-leading order (NLO) to be $\sigma_{st} = 2.86 \pm 0.36$ pb [4]. The small signal cross section and the presence of only one top quark in the final state make the separation of the signal from the large background challenging. Since the signal has very similar final states to the standard model Higgs boson production process $WH \rightarrow \ell\nu b\bar{b}$, the methods of this analysis can be used to search for the Higgs boson.

Recently, the D0 collaboration has reported evidence for single-top-quark production using 0.9 fb^{-1} of data [5] while measuring a cross section of $\sigma_{\mathrm{st}} = 4.7 \pm 1.3$ pb. This Letter reports a significantly more precise measurement of σ_{st} in 2.2 fb^{-1} of $p\bar{p}$ collisions at $\sqrt{s} = 1.96$ TeV using the CDF II detector.

The CDF II detector [6] is a general purpose apparatus located at the Tevatron collider at Fermilab. The detector consists of a solenoidal charged particle spectrometer which includes a silicon microstrip detector array surrounded by a cylindrical drift chamber in a 1.4 T axial magnetic field. The energies of electrons and jets are measured with segmented sampling calorimeters. Surrounding the calorimeters are layers of steel instrumented with planar drift chambers and scintillators used for muon identification.

Three distinct trigger algorithms are employed to select the data used in this analysis: a high p_T electron trigger, a high p_T muon trigger, and a trigger that requires large missing transverse energy with either an energetic electromagnetic cluster or two separated jets [7,8].

Events are further selected by requiring the presence of an isolated electron or muon candidate with $p_T > 20$ GeV/c, large missing transverse energy $\not\!\!E_T > 25$ GeV, and either two or three jets each with $E_T > 20$ GeV and $|\eta| < 2.8$. The jets are identified by a fixed-cone algorithm with radius $\Delta R \equiv \sqrt{(\Delta\eta)^2 + (\Delta\phi)^2} = 0.4$, and their energies are corrected for instrumental effects [9]. At least one of the jets is required to have a displaced vertex (b tag) as identified by the SECVTX algorithm [10]. This b tag preferentially selects jets containing B hadrons.

In order to reduce the Z + jets, $t\bar{t}$, and diboson backgrounds, candidate events with a second charged lepton are rejected. Cosmic ray and photon candidates are identified and removed. Multijet background events without a leptonic W decay ("non-W") are rejected with specific selection requirements [11,12].

The diboson (WW, WZ, ZZ) and $t\bar{t}$ event yields are predicted using PYTHIA [13] Monte Carlo (MC) samples normalized to theoretical cross sections [14,15]. The processes in which a vector boson is produced in association with one or more jets (Z or W + jets) are generated with ALPGEN [16] using PYTHIA's parton showering and underlying event model. The W + jets samples are normalized to the measured data using events with exactly one, two, or three jets. A normalization factor of 1.4 ± 0.4 is applied to ALPGEN's prediction for the fraction of $Wb\bar{b}$ and $Wc\bar{c}$ events. This factor is estimated by comparing the flavor content in b-tagged $W + 1$ jet events in the data to the prediction from simulation. The background from events with mistakenly b-tagged light-flavor jets (Wjj) is estimated by measuring the rate of such mistags in multijet data [10]. The mistag rate is then applied to the W + jets data samples before b tagging. The contributions to the data samples from non-Wjj sources are subtracted from the prediction [17]. Multijet non-W events typically have less $\not\!\!E_T$ than events containing W bosons. By using templates for non-W and W + jets, we fit the $\not\!\!E_T$ distribution and extract the non-W fraction in the high $\not\!\!E_T$ signal region. The kinematic properties of the non-W events are modeled using data events and W + jets is modeled using MC simulated events. The observed event yields and corresponding predictions are given in Table I.

Single top events are simulated using the tree-level matrix-element generator MADEVENT [18]. The two t-channel processes of Figs. 1(a) and 1(b) are combined to match the event kinematics as predicted by a fully differential NLO calculation [4,19].

The expected standard model signal-to-background ratio for selected events is ~7% in the two-jet sample and ~5% in the three-jet sample. The uncertainties on the back-

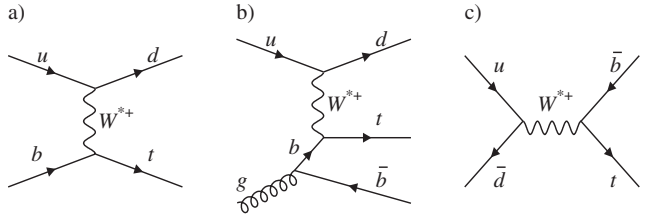

FIG. 1. Representative Feynman diagrams of single-top-quark production. (a) and (b) are t-channel processes, and (c) is the s-channel process.

TABLE I. Background composition and predicted number of single top events in 2.2 fb^{-1} of CDF Run II data with at least one b-tagged jet.

Process	W + 2 jets	W + 3 jets
s-channel signal	40.3 ± 5.8	13.1 ± 1.9
t-channel signal	60.8 ± 8.9	17.9 ± 2.6
$Wb\bar{b}$	451.1 ± 136.0	138.0 ± 41.7
$Wc\bar{c} + Wcj$	372.5 ± 114.8	103.2 ± 31.8
Wjj	337.1 ± 41.9	101.6 ± 12.8
$t\bar{t}$	142.0 ± 20.3	327.8 ± 46.6
Non-W	60.5 ± 24.2	21.0 ± 8.4
Diboson	61.1 ± 6.2	20.4 ± 2.1
Z + jets	25.5 ± 3.8	10.5 ± 1.5
Total prediction	1550.9 ± 256.6	753.5 ± 87.6
Observed	1546	719

ground predictions are larger than the expected signals; therefore, we have developed three powerful discriminants to distinguish signal from background events. The predicted distributions of each discriminant are fit to the data to extract the single top production cross section. All analyses use the same event selection and were optimized with the signal region blinded.

Wjj, $Wc\bar{c}$, and Wcj events do not contain b-quark jets, but constitute ~40% of the estimated background after imposing a b tag requirement. As part of all three discriminants we employ a jet-flavor separating variable, b_{nn}, constructed using the neural network tool NEUROBAYES [20], which is trained to distinguish b jets from charm and light-flavor jets based on secondary vertex tracking information [11]. The usage of b_{nn} leads to an improvement in sensitivity of 15 to 20% in each analysis.

Likelihood function discriminant (LF).—A projective likelihood technique [17,21] is used to combine information from several input variables to optimize the separation of the single top signal from the backgrounds. Two likelihood functions are created, one for two-jet events, $\mathcal{L}_{2j}$, and one for three-jet events, $\mathcal{L}_{3j}$. The input variables used for $\mathcal{L}_{2j}$ are b_{nn}, $Q \times \eta$ [22], the invariant mass of the $\ell\nu b$ system $M_{\ell\nu b}$, the total scalar sum of transverse energy in the event H_T, $\cos\theta^*_{\ell j}$ [23], the dijet mass M_{jj}, and the t-channel matrix element. The matrix element used here is computed using four-vectors from the event after kinematically constraining $M_{\ell\nu} = M_W$ and $M_{\ell\nu b} = m_t$, where M_W and m_t are the W and top quark pole masses in the matrix element. The M_W constraint introduces a quadratic ambiguity in the z component of the neutrino momentum; we choose the solution with the smaller $|p_z^\nu|$.

For events with three jets, ten input variables are used to construct $\mathcal{L}_{3j}$: b_{nn}, $Q \times \eta$, $M_{\ell\nu b}$, $\cos\theta^*_{\ell j}$, M_{jjn} of the two jets not selected as the b from top decay, the number of b tags, the smallest ΔR between any two jets, the smallest p_T of the three jets, $p_T(W)$, and E_T of the jet selected as coming from the b from the top quark decay. The b-quark jet is chosen using a linear combination of the jet E_T and the χ^2 resulting from the comparison of the kinematically constrained jet energy and the measured jet energy.

Matrix-element discriminant (ME).—The matrix-element method relies on the evaluation of event probability densities for signal and background processes based on calculations of the standard model differential cross sections [12,24]. We construct these probability densities for each process for each event given their measured quantities x by integrating the appropriate differential cross section $d\sigma(y)/dy$ over the underlying partonic quantities y, convolved with the parton distribution functions (PDFs) and detector resolution effects:

$$P(x) = \sum_{\text{perm.}} \int \frac{d\sigma(y)}{dy} f(q_1) f(q_2) dq_1 dq_2 W(x, y) dy. \quad (1)$$

The PDFs ($f(q_1)$ and $f(q_2)$) take into account the flavors of the colliding quark and antiquark. We use the CTEQ PDF parameterization [25]. The detector resolution effects are described by a transfer function $W(x, y)$ relating x to y. The momenta of electrons, muons, and the angles of jets are assumed to be measured exactly. $W(x, y)$ maps parton energies to measured jet energies after correction for instrumental effects [9]. This mapping is obtained by parameterizing the jet response in fully simulated MC events. The definition of the probability densities includes possible permutations of matching jets with partons. The integration is performed over the energy of the partons and p_z^ν. We calculate the matrix element for the event probability at tree-level using MADGRAPH [26]. Event probability densities are computed for the s-channel and t-channel signal as well as $Wb\bar{b}$, $Wc\bar{c}$, Wcj, Wjj, and $t\bar{t}$ background hypotheses. In the specific case of the $t\bar{t}$ matrix element, additional integrations are performed over the momenta of particles not detected.

The event probability densities are combined into an event probability discriminant: $\text{EPD} = P_{\text{signal}}/(P_{\text{signal}} + P_{\text{background}})$. To better classify signal events that contain b jets, we incorporate the output b_{nn} of the neural network jet-flavor separator into the final discriminant:

$$\text{EPD} = \frac{b_{nn} P_{st}}{b_{nn}(P_{st} + P_{t\bar{t}} + P_{Wb\bar{b}}) + (1 - b_{nn})(P_{Wc\bar{c}} + P_{Wcj} + P_{Wjj})}. \quad (2)$$

Both signal channels are combined to one single top probability density $P_{st} = P_{s\text{-channel}} + P_{t\text{-channel}}$.

Neural network discriminant (NN).—The third multivariate approach [11] employs neural networks, which have the general advantage that correlations between the discriminating input variables are identified and utilized to optimize the separation power between signal and background. The networks are developed using the NEUROBAYES analysis package [20], which combines a three-layer feed-forward neural network with a complex and robust preprocessing of the input variables. Bayesian regularization techniques are utilized to avoid overtraining.

Four separate networks are trained to identify different signals in distinct samples using simulated events from the common samples described previously. An s-channel signal is used for training on events with two b-tagged jets. A t-channel signal is used for the two-jet sample with a single b tag and for the three-jet samples with one or two b tags. The networks use 11 to 18 input variables. The most important ones are $M_{\ell\nu b}$, b_{nn}, M_{jj}, $Q \times \eta$, $\cos\theta^*_{\ell j}$, the transverse mass of the W boson, and H_T. The input variables are selected from a large list using an automated evaluation during the preprocessing step before the network training. In an iterative process, we determine those variables whose removal would cause a significant loss in separation power between signal and background and use them for network training.

Combination.—We studied two methods to combine the cross section fit results. The best linear unbiased estimator (BLUE) [27] technique optimizes the coefficients of a linear combination using the uncertainties and correlations of the three individual analyses: LF, ME, and NN. The correlation coefficients between the analyses are: LF-ME: 59%; LF-NN: 74%; ME-NN: 61%. In another combination approach, a "super analysis" is built based on the outcomes for each event in each of the three individual analyses. The superdiscriminant method uses a neuro-evolution network [28] trained to separate the signal from the background based on the discriminant outputs of the three analyses. With the superdiscriminant analysis we improve

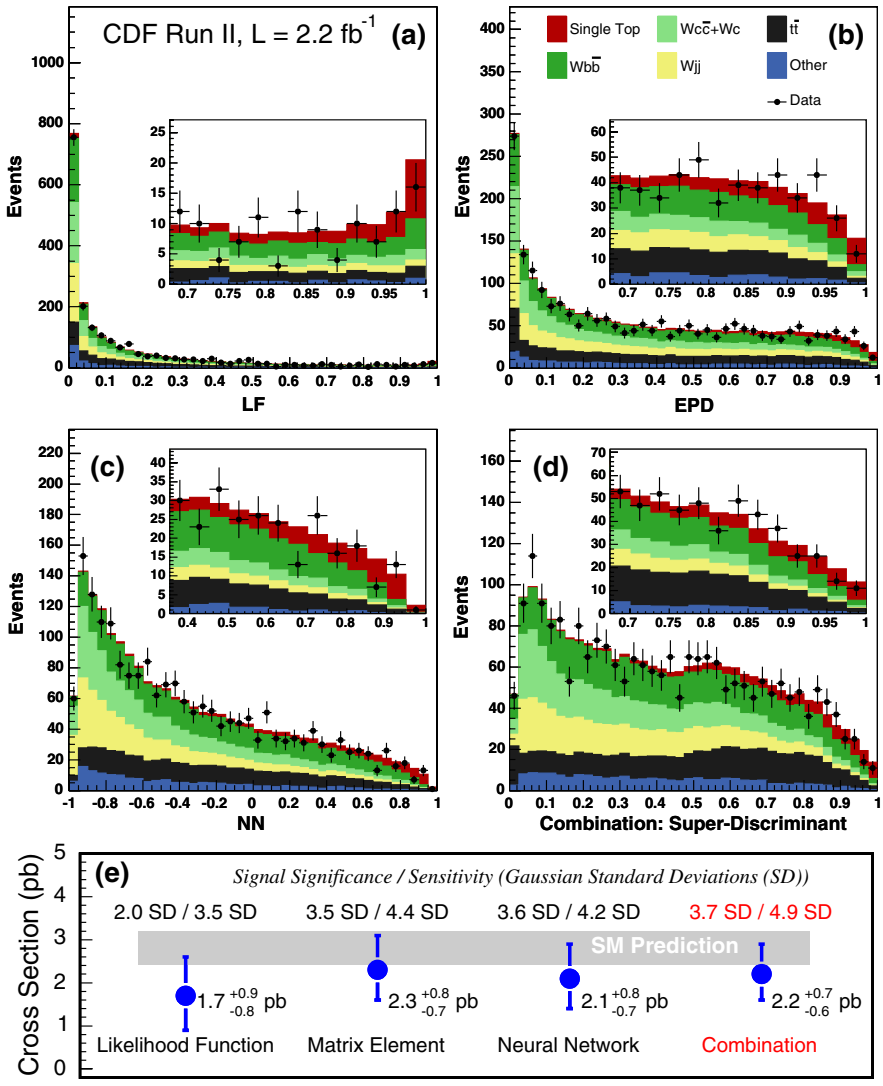

FIG. 2 (color online). Discriminant distribution for all channels combined of the (a) LF analysis, (b) ME analysis, (c) NN analysis and (d) combined superdiscriminant analysis. Points with error bars indicate the data. The predicted signal and background distributions are shown as stacked histograms. The insets show the candidate events in the signal regions. A summary of all results is shown in (e).

the sensitivity by 10% over the best individual analysis, and we use it to quote our final results. As a cross-check, BLUE yields a 7% sensitivity improvement.

Before unblinding the data, the MC simulation of each input variable and the discriminant outputs were checked in data control samples depleted in signal. These are the lepton $+b$-tagged four-jet sample, which is enriched in $t\bar{t}$ events, and the two- and three-jet samples in which no jet is b tagged. The latter are high-statistics samples with similar kinematics to the b-tagged signal samples. The data distributions in the control samples are described well by the MC simulation.

Figure 2 shows the distributions of the individual analyses' discriminants and the superdiscriminant. We calculate the probability (p-value) [2] of the background-only discriminant distribution to fluctuate to the observed data or more which is then converted into signal significance under a Gaussian assumption. All sources of systematic uncertainty are included and correlations between normalization and discriminant shape changes are considered. Uncertainties in the jet energy scale, b-tagging efficiencies, lepton identification and trigger efficiencies, the amount of initial and final state radiation, PDFs, factorization and renormalization scale, and MC modeling have been explored and incorporated in this combination and all individual analyses.

We interpret the excess of signal-like events over the expected background as strong evidence for single top production with a signal significance of 3.7 standard deviations, with a sensitivity, defined to be the median expected significance, of 4.9 standard deviations. The most probable value of the combined s-channel and t-channel cross sections is $\sigma_{st} = 2.2^{+0.7}_{-0.6}$ pb for a top quark mass of 175 GeV/c^2 which is consistent with the cross-check result, obtained from BLUE, $\sigma_{st} = 2.3 \pm 0.7$ pb. The dependence on the top quark mass is $+0.02$ pb/(GeV/c^2). From the cross section measurement at $m_t = 175$ GeV/c^2, we obtain $|V_{tb}| = 0.88^{+0.13}_{-0.12}(\text{stat} + \text{syst}) \pm 0.07$ (theory [4]) and limit $|V_{tb}| > 0.66$ at the 95% C.L. assuming a flat prior in $|V_{tb}|^2$ from 0 to 1. This is the most precise direct measurement of $|V_{tb}|$ to date.

We thank the Fermilab staff and the technical staffs of the participating institutions for their vital contributions. This work was supported by the U.S. Department of Energy and National Science Foundation; the Italian Istituto Nazionale di Fisica Nucleare; the Ministry of Education, Culture, Sports, Science and Technology of Japan; the Natural Sciences and Engineering Research Council of Canada; the National Science Council of the Republic of China; the Swiss National Science Foundation; the A. P. Sloan Foundation; the Bundesministerium für Bildung und Forschung and the Alexander von Humboldt Foundation, Germany; the Korean Science and Engineering Foundation and the Korean Research Foundation; the Science and Technology Facilities Council and the Royal Society, UK; the Institut National de Physique Nucleaire et Physique des Particules/CNRS; the Russian Foundation for Basic Research; the Ministerio de Educación y Ciencia and Programa Consolider-Ingenio 2010, Spain; the Slovak R&D Agency; and the Academy of Finland.

[a]Deceased.
[b]Universiteit Antwerpen, B-2610 Antwerp, Belgium
[c]Visiting scientist from Chinese Academy of Sciences, Beijing 100864, China.
[d]Visiting scientist from University of Bristol, Bristol BS8 1TL, United Kingdom.
[e]Visiting scientist from University of California Irvine, Irvine, CA 92697, USA.
[f]Visiting scientist from University of California Santa Cruz, Santa Cruz, CA 95064, USA.
[g]Visiting scientist from Cornell University, Ithaca, NY 14853, USA.
[h]Visiting scientist from University of Cyprus, Nicosia CY-1678, Cyprus.
[i]Visiting scientist from University College Dublin, Dublin 4, Ireland.
[j]Visiting scientist from University of Edinburgh, Edinburgh EH9 3JZ, United Kingdom.
[k]Visiting scientist from Universidad Iberoamericana, Mexico D.F., Mexico.
[l]Visiting scientist from University of Manchester, Manchester M13 9PL, United Kingdom.
[m]Visiting scientist from Nagasaki Institute of Applied Science, Nagasaki, Japan.
[n]Visiting scientist from University de Oviedo, E-33007 Oviedo, Spain.
[o]Visiting scientist from Queen Mary, University of London, London, E1 4NS, United Kingdom.
[p]Visiting scientist from Texas Tech University, Lubbock, TX 79409, USA.
[q]Visiting scientist from IFIC(CSIC-Universitat de Valencia), 46071 Valencia, Spain.
[r]Visiting scientist from Istituto Nazionale di Fisica Nucleare, Sezione di Cagliari, 09042 Monserrato (Cagliari), Italy.

[1] F. Abe *et al.* (CDF Collaboration), Phys. Rev. Lett. **74**, 2626 (1995); S. Abachi *et al.* (D0 Collaboration), *ibid.* **74**, 2632 (1995).
[2] C. Amsler *et al.* (Particle Data Group), Phys. Lett. B **667**, 1 (2008).
[3] D. Acosta *et al.* (CDF Collaboration), Phys. Rev. Lett. **95**, 102002 (2005).
[4] B. W. Harris *et al.*, Phys. Rev. D **66**, 054024 (2002); Z. Sullivan, *ibid.* **70**, 114012 (2004).
[5] V. M. Abazov *et al.* (D0 Collaboration), Phys. Rev. Lett. **98**, 181802 (2007); V. M. Abazov *et al.* (D0 Collaboration), Phys. Rev. D **78**, 012005 (2008).
[6] D. Acosta *et al.* (CDF Collaboration), Phys. Rev. D **71**, 032001 (2005).

[7] We use a cylindrical coordinate system with its origin in the center of the detector, where θ and ϕ are the polar and azimuthal angles, respectively, and pseudorapidity is $\eta = -\ln\tan(\theta/2)$. The missing E_T ($\not\!\!E_T$) is defined by $\vec{\not\!\!E}_T = -\sum_i E_T^i \hat{n}_i$, i = calorimeter tower number, where $\hat{n}_i$ is a unit vector perpendicular to the beam axis and pointing at the ith calorimeter tower. $\vec{\not\!\!E}_T$ is corrected for high-energy muons and also jet energy corrections. We define $\not\!\!E_T = |\vec{\not\!\!E}_T|$. The transverse momentum p_T is defined to be $p\sin\theta$.

[8] A. Abulencia *et al.* (CDF Collaboration), Phys. Rev. D **74**, 072006 (2006); T. Aaltonen *et al.* (CDF Collaboration), Phys. Rev. Lett. **100**, 211801 (2008).

[9] A. Bhatti *et al.*, Nucl. Instrum. Methods Phys. Res., Sect. A **566**, 375 (2006).

[10] D. Acosta *et al.*, Phys. Rev. D **71**, 052003 (2005).

[11] S. Richter, Ph.D. thesis, University of Karlsruhe, Report No. FERMILAB-THESIS-2007-35, 2007.

[12] P. Dong, Ph.D. thesis, University of California, Los Angeles, Report No. FERMILAB-THESIS-2008-12, 2008.

[13] T. Sjöstrand *et al.*, Comput. Phys. Commun. **135**, 238 (2001).

[14] R. Bonciani *et al.*, Nucl. Phys. **B529**, 424 (1998); M. Cacciari *et al.*, J. High Energy Phys. 04 (2004) 068.

[15] J. M. Campbell and R. K. Ellis, Phys. Rev. D **60**, 113006 (1999).

[16] M. L. Mangano *et al.*, J. High Energy Phys. 07 (2003) 001; M. L. Mangano *et al.*, Nucl. Phys. **B632**, 343 (2002); F. Caravaglios *et al.*, Nucl. Phys. **B539**, 215 (1999).

[17] S. Budd, Ph.D. thesis, University of Illinois at Urbana-Champaign, Report No. FERMILAB-THESIS-2008-41, 2008.

[18] J. Alwall *et al.*, J. High Energy Phys. 09 (2007) 028.

[19] J. Lück, Diplom thesis, University of Karlsruhe, Report No. FERMILAB-MASTERS-2006-01, 2006.

[20] M. Feindt and U. Kerzel, Nucl. Instrum. Methods Phys. Res., Sect. A **559**, 190 (2006).

[21] K. Ackerstaff *et al.* (OPAL Collaboration), Eur. Phys. J. C **1**, 425 (1998).

[22] $Q \times \eta$ is the charge of the lepton times the pseudorapidity of the jet not assigned to be the b from top decay. C.-P. Yuan, Phys. Rev. D **41**, 42 (1990).

[23] $\cos\theta^*_{\ell j}$ is the cosine of the angle between the lepton and the jet not assigned to be the b from top decay, in the top quark rest frame. G. Mahlon and S. J. Parke, Phys. Rev. D **55**, 7249 (1997).

[24] B. Stelzer, Ph.D. thesis, University of Toronto, Report No. FERMILAB-THESIS-2005-79, 2005; F. Canelli, Ph.D. thesis, University of Rochester, Report No. FERMILAB-THESIS-2003-22, 2003.

[25] J. Pumplin *et al.*, J. High Energy Phys. 07 (2002) 012.

[26] F. Maltoni and T. Stelzer, J. High Energy Phys. 02 (2003) 027.

[27] L. Lyons *et al.*, Nucl. Instrum. Methods Phys. Res., Sect. A **270**, 110 (1988).

[28] K. O. Stanley and R. Miikkulainen, Evolutionary Computation **10**, No. 2, 99 (2002).